https://doi.org/10.5194/hess-2022-124
Preprint. Discussion started: 1 April 2022

Hydrology and Earth System Sciences
Discussions

Global assessment of sub-national drought impact based on the Geocoded Disasters dataset and land reanalysis

Yuya Kageyama[1], Yohei Sawada[1]

[1]Institute of Engineering Innovation, The University of Tokyo, Tokyo, 113-8656, Japan

Correspondence to: Yuya Kageyama (ykageyama21@gmail.com)

Abstract. Despite the importance of a linkage between hydro-meteorological drought hazards and their socio-economic impact, the linkage at a sub-national level has yet to be evaluated due to the lack of precise sub-national information on disaster locations. Using the newly developed Geocoded Disasters (GDIS) dataset, we examined whether the sub-national socio-economic drought information could be represented by hydro-meteorological hazards quantified from soil moisture in ERA5-Land during 1964–2018. We found that ERA5-Land soil moisture accurately captured the socio-economic impacts of drought shown in GDIS. Our comparison between GDIS and ERA5-Land can quantify vulnerability to drought, and we found that Sub-Saharan Africa and South Asia were vulnerable to drought while North America and Europe were robust to drought. Both GDIS and ERA5-Land indicated that the Horn of Africa, northern China, and western India were drought-prone areas. Since it is difficult for national-level analyses to accurately identify the locations of drought-prone areas especially in large countries such as China and India, our analysis clarifies the importance of the use of the sub-national disaster information.

1 Introduction

Drought is one of the costliest natural disasters with cascading impacts on multiple socio-economic sectors (Mishra and Singh, 2010). Wilhite and Glantz (1985) proposed a conceptual model of drought propagation, from natural hydro-meteorological hazards defined by physical characteristics (e.g., precipitation, soil moisture, or streamflow) to socio-economic drought impacts (e.g., crop yield loss, water shortage, or health problem). The propagation from the natural hydro-meteorological hazards to the socio-economic impact can be affected by many regional vulnerability factors, such as infrastructure, economic, social, or cultural assets (e.g., Fuchs et al., 2019; Lavell et al., 2012; UNDP, 2004; Wilhite and Glantz, 1985). To understand this drought propagation, a sub-national level disaster analysis is necessary, rather than aggregated national level disaster analyses (Rosvold and Buhaug, 2021). How historical drought events evolved from natural hydro-meteorological hazards to socio-economic drought impacts at a sub-national level needs to be analyzed to improve regional drought mitigation measures.

https://doi.org/10.5194/hess-2022-124
Preprint. Discussion started: 1 April 2022


Hydrology and Earth System Sciences
Discussions

Several studies have analyzed the linkage between natural hydro-meteorological hazards and socio-economic drought impacts to quantify the regional characteristics of historical drought events. Disaster databases such as the Emergency Events Database EM-DAT (Guha-Sapir et al., 2022), the European Drought Impact report Inventory (EDII) (Stahl et al., 2016), US Drought Impact Reporter (US DIR) (Wilhite et al., 2007), as well as newspaper information (de Brito et al., 2020) have been used as reference data of historical socio-economic impacts. Bachmair et al. (2016) used EDII to estimate the thresholds of hydro-meteorological drought indices at which socio-economic droughts occur in Germany and UK at a sub-national level. Noel et al. (2020) compared the U.S. Drought Monitor (USDM) (Svoboda et al. 2002), a weekly map depicting severity and spatial extent of drought, with US DIR at the state level. Although EDII and US DIR contain detailed disaster information at a sub-national level and are useful to quantify the linkage between hydro-meteorological hazards and socio-economic impacts, they do not cover the entire globe. EM-DAT is a global database and has been extensively used for the international comparison of disaster risks and vulnerability (e.g., Jägermeyr et al., 2018; Shen and Hwang, 2019; Tschumi and Zscheischler, 2020). Although some studies used text-based disaster locations (i.e., names of affected provinces, districts, and towns) in EM-DAT to perform the sub-national scale analyses, they simply evaluated the applicability of a drought index for the specific regional events (e.g., Bayissa et al., 2018; Lu et al., 2019) and for global events in a short period of time (2010–2015) (Sánchez et al., 2018). The sub-national information of the disaster database has not been fully used to quantify the linkage between hydro-meteorological drought hazards and socio-economic impacts in a global scale. In addition, regional vulnerability against drought events has not been quantified by using such database in a global scale.

Instead of the disaster databases, agricultural production or remotely sensed vegetation dynamics have also been used to assess the impact of drought on society. Udmale et al. (2020) compared cereal production with drought indices such as Standardized Precipitation Index (SPI) (McKee et al., 1993) and Standardized Precipitation Evaporation Index (SPEI) (Vicente-Serrano et al., 2010) in India. Kim et al. (2019) examined the vulnerability of cereal production to drought in a country scale using a global crop model. Chen et al. (2020) quantified the impact of droughts on vegetation growth for different biome types and climate regimes by comparing SPEI and a vegetation index. Although agricultural production and vegetation dynamics are available globally and easy to be quantified, there are some problems to use them as reference data of socio-economic drought impacts. Agricultural production can be affected by factors other than drought and it can capture aggregated information on large events (Bachmair et al., 2016). It is unclear whether socio-economic drought impacts are associated with declined vegetation growth. It is ideal to treat the socio-economic drought impact in terms of whether this is socially perceived as drought.

The linkage between natural hydro-meteorological hazards and socio-economic drought impact at a sub-national level has yet to be globally evaluated. The major obstacle is a lack of accurate information of socio-economic drought impacts in sub-national scales (Bachmair et al., 2016). Recently, a global dataset of geocoded disaster locations, the Geocoded DISasters (GDIS), has been developed (Rosvold and Buhaug, 2021). Although EM-DAT contains information about the location of

https://doi.org/10.5194/hess-2022-124
Preprint. Discussion started: 1 April 2022


Hydrology and Earth System Sciences
Discussions

disasters, they are text-based information and some events have incomplete information about their locations, which is not suitable for comprehensive geospatial analyses. GDIS is the geocoded database based on the EM-DAT's location information with some manual validations and provides GIS polygons of affected administrative units. GDIS can be a useful tool to globally assess the linkage between natural hydro-meteorological hazards and socio-economic drought impact with precise locations at a sub-national level.

This study aims to examine the linkage between natural hydro-meteorological hazards and the sub-national socio-economic drought impact shown in GDIS. As a natural hydro-meteorological hazard, we used drought indices generated from soil moisture simulated by land reanalysis, ERA5-Land (Muñoz-Sabater, 2019; Muñoz-Sabater, 2021). First, we examined whether the reanalysis product could capture the socio-economic impacts in GDIS. Then, we quantified the vulnerability to drought in different geographical regions. Finally, we compared the global spatial distribution of drought-prone areas in GDIS with those quantified from ERA5-Land.

2 Data

2.1 ERA5-Land

To calculate drought indices, ERA5-Land soil moisture data were used. Wilhite and Glanz (1985) mentioned that soil moisture plays an important role in the drought propagation since it affects both agricultural and hydrological aspects of drought (see also Sawada (2018)). Many drought monitoring systems have also used soil moisture as one of the most important variables (e.g., USDM, Svoboda et al., 2002; The German drought monitor, Zink et al., 2016; InterSucho in Czech Republic and Slovakia, Trnka et al., 2020).

We used monthly averaged data from 1950 to 2020. The original spatial resolution of 0.1° was upscaled to 0.25° to reduce the data volume, by using a remap function of the Climate Data Operators (CDO) version 2.0.0 (Schulzweida, 2021). This spatial resolution is relatively high compared to the previous global-scale drought studies (e.g., Hanel et al., 2018; Herrera-Estrada et al., 2017; Mocko et al., 2021; Sawada, 2018).

We used the first (0–7 cm), second (7–28 cm), and third (28–100 cm) layers' soil moisture in ERA5-Land to generate drought indices. Since previous works used soil moisture from the top to 1–2 m soil depths as root zone soil moisture (e.g., Almendra-Martín et al., 2021; Hanel et al., 2018; Herrera-Estrada et al., 2017; Mocko et al., 2021), we also used the top 1 m (0–100 cm) soil moisture data. For the top 1 m soil moisture, we calculated the weighting average of soil moisture in the first, second, and third layers according to their thicknesses.

https://doi.org/10.5194/hess-2022-124
Preprint. Discussion started: 1 April 2022


Hydrology and Earth System Sciences
Discussions

2.2 GDIS

GDIS (Rosvold and Buhaug, 2021) can be downloaded from https://cmr.earthdata.nasa.gov/search/concepts/C2022273992-SEDAC.html (data downloaded for this study: October 2021). GDIS is the geocoded disaster locations database based on EM-DAT. A natural disaster is recorded into EM-DAT if at least one of the following criteria is fulfilled: 10 or more people dead; 100 or more people affected; the declaration of a state of emergency, and a call for international assistance (Guha-Sapir et al., 2022).

The 282 drought events from 1964 to 2018 were analyzed. Each drought event is distinguished based on the EM-DAT database's event identifier (*disasterno*). In EM-DAT, disaster events are uniquely distinguished by the combination of an 8-digit disaster code and a 3-digit country code. In contrast, GDIS uses only the 8-digit disaster code, which is common with EM-DAT, and assigns the same identifier to a disaster event even if it spreads over multiple countries. In the case of extensive drought events, such as ones induced by El Niño, it is not reasonable to treat distant countries with the same event identifier. In this study, the event classification of the original EM-DAT was adopted, so that events with the same disaster code that spread over multiple countries in GDIS were analyzed as a separate event for each country. Drought events in GDIS that met the following criteria were used in this study: (1) The drought period is longer than or equal to two months and (2) The GDIS event area is larger than or equal to 50 grid cells in the upscaled ERA5-Land. We did not analyze flash drought, which occurred in shorter than two months. The effective resolution of the phenomena that can be represented by a numerical simulation model is several times as large as the original size of computational grids (Skamarock, 2004), so that the events with the small extent relative to the grid spacing were neglected in this study. GDIS itself does not have drought period information, namely when the event starts and ends. The drought period information was added to GDIS via EM-DAT database's event identifiers. EM-DAT shows only the event year and provides no information on the start and/or end month for some drought events. In such cases, we applied January for the start and December for the end of the event. GDIS provides affected spatial geometry in the form of GIS polygons of administrative units. Administrative units with the same event identifier (*disasterno*) were treated as one "GDIS event area" (see Fig. 2 as an example). Sánchez et al. (2018) treated one drought event per one administrative unit. However, this event classification depends on the fineness of the division of administrative units (e.g., Thailand, where administrative units are very finely divided, has more than 50 events during 2010–2015 in Sánchez et al. (2018)), which affects the results of drought detection skill. Therefore, we treated administrative units with the same event identifier as one drought event, following EM-DAT classification.

2.3 Other supporting data

To show the drought vulnerability by geographical regions, we used the classification of the world bank geographical regions.

https://doi.org/10.5194/hess-2022-124
Preprint. Discussion started: 1 April 2022


Hydrology and Earth System Sciences
Discussions

As land cover data, we used the MODIS land cover climate modeling grid (MCD12C1) version 6 data product (Friedl and Sulla-Menashe, 2015). This land cover product has 17 classes. The temporal resolution is yearly, and we used the latest, 2020 data. The original spatial resolution is 0.05° and we resampled it to 0.25° by the nearest neighbour approach.

3 Methodology

3.1 Drought indices

We used two drought indices, the Drought Area Percentage (DAP) and the Standardized Deficit Index (SDI), to evaluate the severity of the hydro-meteorological drought hazard in ERA5-Land. For the soil moisture data in each grid cell, percentiles were first calculated for each calendar month separately during 1950–2020. After the percentiles were calculated, only data during the period with the GDIS drought events (1964–2018) was used in all subsequent steps of this study. The 20th percentile was taken as a threshold for defining a drought at each grid cell (Sheffield and Wood, 2011; Hanel et al., 2018). DAP is the maximum percentage of the area where soil moisture is below the 20th percentile threshold within the GDIS event area during the GDIS drought period. The higher the percentage means the severer the hydro-meteorological hazard is. DAP has been used as a drought index in many studies (e.g., Sánchez et al. 2018; Udmale et al. 2020).

DAP is a snapshot of the long-lasting drought phenomenon and does not include the cumulative effects of the long-lasting drought. The other limitation of DAP is that it could be affected by the size of the GDIS event area; DAP tends to be small in large event areas. In addition to DAP, we developed a new drought indicator, called SDI, which accounts for the cumulative effects of drought and is less influenced by the size of the GDIS event area. First, a deficit volume, a cumulative deviation below the 20th percentile threshold, was calculated for each grid cell. Then, we summed up the maximum annual deficit volume per grid cell in each GDIS event area, which is defined as the annual maximum deficit volume in the GDIS event area. The cumulative effect of the movement of drought areas can be considered by calculating the annual maximum value for each grid before averaging the values within the GDIS event area. Finally, the annual maximum deficit volume in the GDIS event area was standardized, dividing each year's annual maximum deficit volume by the mean of the annual maximum deficit volume over the period (1964–2018). The higher SDI means the severer hydro-meteorological hazard, and the value of 1 is the standard annual maximum drought event. The standardization makes it possible to compare the different events across space and time, even if the size of the GDIS event area is quite different. Hanel et al. (2018) calculated SDI for each grid cell. We extended this methodology to evaluate the drought index representative in the GDIS event area.

3.2 Evaluation of the drought indices by GDIS

To evaluate whether the drought indices can accurately identify the drought events shown in GDIS, we tested whether the drought indices during the GDIS drought period were distinguishable from those during the whole period (1964–2018). We applied a bootstrap random resampling method to show the distributions of drought indices for the whole period. For DAP,

https://doi.org/10.5194/hess-2022-124
Preprint. Discussion started: 1 April 2022


Hydrology and Earth System Sciences
Discussions

we set a 12-month moving window, which is approximately the mean of the drought duration in GDIS, and extracted the maximum percentage in each window for each GDIS event. From this assemblies, we extracted DAP randomly with 1000 replications. For SDI, we extracted SDI randomly with 1000 replications from the whole study period. We used two-sample Kolmogorov–Smirnov (*K*–*S*) test (Massey, 1951) to quantify the difference of the distributions of drought indices during the GDIS drought period and the whole period. If the *p*-value of *K*–*S* test is smaller than 0.01, the hypothesis that two distributions follow the same distribution is rejected at 1% significance level. Due to the difference of the sample size (i.e., Drought period: 282; Whole period by a bootstrap random resampling method: 1000), the distributions were normalized, namely the densities sum to 1, prior to the comparison. We recognized that the drought indices successfully capture the GDIS drought events if the two distributions are not statistically the same.

3.3 Regional vulnerability to drought

The levels of hydro-meteorological drought indices associated with socio-economic drought events identified in GDIS are different in different regions due to a wide variety of vulnerability to drought. Following Bachmair et al. (2016), the levels of SDI which are associated with socio-economic drought events in GDIS were quantified and analyzed. The levels of SDI were stratified by geographical regions to understand the distribution of vulnerability in each region.

3.4 Global drought frequency analysis by drought clustering

We analyzed whether drought-prone areas identified by drought indices are globally consistent with those found in GDIS. We applied the drought clustering method (Andreadis et al., 2005) to search for the spatially contiguous areas (or clusters) under drought at each timestep. In this drought clustering, we assume that drought occurs over a reasonably large spatial area driven by a large-scale climate process (Sheffield and Wood, 2011). We used the processing code developed by Herrera-Estrada and Diffenbaugh (2020).

After the percentiles are calculated in each grid cell, a 2-D median filter is applied to each monthly global data to smooth out small-scale noise. Contiguous areas under drought (soil moisture below the 20th percentile in this study) are aggregated into clusters at each timestep. Following Herrera-Estrada and Diffenbaugh (2020), we analyzed clusters that reach a maximum area of at least 100,000 km^2 (approximately 120 grid cells in the upscaled ERA5-Land) to focus on large-scale droughts. The location of the cluster centroid is detected at each time step using the weighting average of the cluster's location with the intensity values of the cluster grid cells. Droughts whose centroids fell within the barren or sparsely vegetated areas based on MODIS land cover were masked out from the cluster analysis, due to the little or no exposure (i.e., population, assets) (e.g., Carrão et al., 2016; Herrera-Estrada et al., 2017). We confirmed that there were no drought events in GDIS which were fully included within the barren or sparsely vegetated areas. Figure 1 demonstrates this drought clustering. The cluster centroid shows the area that experiences higher drought displacement, and we made an upscaled map of cluster centroids from the

https://doi.org/10.5194/hess-2022-124
Preprint. Discussion started: 1 April 2022

original spatial resolution of 0.25° to 2.5°. For a sensitivity analysis of this upscale resolution, see Fig. S1. See Andreadis et al. (2005) for details about the clustering method.

We visualized the socio-economic drought-prone areas by overlaying all polygons of the GDIS. We compared the regional drought frequencies in GDIS with the number of drought cluster centroids by ERA5-Land. We examined whether hydro-meteorological drought-prone areas are consistent with GDIS.

4 Results

4.1 The performance of drought indices to detect the drought

Figure 2 demonstrates DAP and SDI for the drought events in Ethiopia and Argentina in 2009. For both drought indices, higher values indicate severer drought. Figures 2 (a) and 2 (e) show that DAPs in the first and second soil layers respond to rainfall deficit more quickly than the deep soil layers. During the GDIS drought period, all layers show high DAPs, and the third layer has been experiencing a high DAP for a long time. DAPs in the first and second layer are sometimes high outside of the GDIS drought period. Root-zone (0–100 cm) layer generally follows the third layer's fluctuations, though the root-zone positions between the second and third layers during the GDIS drought period in Ethiopia case. Figures 2 (c) and 2 (g) show that SDIs fluctuate less compared with DAPs. This is because SDI considers the cumulative effect. During the GDIS drought period, all layers show high SDIs, and the differences between the GDIS drought period and the non-drought period stand out more prominently compared with DAP. The third layer shows the highest SDI during the GDIS drought period, especially in Argentina case, reflecting the consistently high DAP during the GDIS drought period. Root-zone (0–100 cm) layer generally follows the third layer's fluctuations.

Figures 3 and 4 reveal that ERA5-Land based drought indices can distinguish the GDIS drought period from the whole period. In Fig. 3, DAP during the GDIS drought periods is significantly higher than that of the whole period in all soil layers. Please note that the samples in whole period shown in Fig. 3 include those during the GDIS drought period. In addition, severe drought events unreported in GDIS may also be included. The difference of the median values of DAP in the GDIS drought period and the whole period is largest in the third layer (28–100 cm) case. In Fig. 4, SDI during the GDIS drought period is significantly higher than that of the whole period in all soil layers, as we found in DAP. Although the second, third and root-zone soil layers show the similar distributions, the difference of the median values of SDI in the GDIS drought period and the whole period is largest in the root-zone (0–100 cm) case. Both of drought indices based on ERA5-Land can capture the GDIS drought events. We will use SDI for the regional comparison shown below, because SDI is a standardized indicator, which allows the comparison between the different events across space and time, even if the size of the GDIS event area is substantially different.

https://doi.org/10.5194/hess-2022-124
Preprint. Discussion started: 1 April 2022


Hydrology and Earth System Sciences
Discussions

4.2 Regional vulnerability to drought

Figure 5 shows the distribution of the root-zone layer's soil moisture-based SDI stratified by geographical regions. Sub-Saharan Africa and South Asia have a large number of small SDI events associated with the GDIS identified drought, while North America and Europe have a large number of large SDI events. A large number of small SDI events indicates that less severe hydro-meteorological droughts have caused serious socio-economic impacts, meaning that the regions are vulnerable to drought. On the other hand, the regions with a large number of large SDI events can be recognized as robust regions to drought. Thus, Sub-Saharan Africa and South Asia are vulnerable to drought, while North America and Europe are robust to drought. This regional characteristic of vulnerability to drought can be found when SDI is generated by soil moisture in different soil layers (not shown). Note that Middle East & North Africa were excluded from the analysis because the sample size was too small (n = 4).

4.3 Global drought frequency analysis by drought clustering

Figure 6 shows the number of drought events at a sub-national level during 1964–2018 based on GDIS. It shows that the Horn of Africa, Mozambique, northern China, and western India are socio-economic drought-prone areas. Each region is shown enlarged in Figs. 6 (b) to (e). Figure 7 shows the number of drought events on the aggregated national level during the same period based on EM-DAT. Although we can see that the number of drought events is high in China, there is little information about the regional differences in drought-prone areas.

This distribution of drought-prone areas in GDIS can be reproduced by ERA5-Land. Figure 8 shows the number of the drought cluster centroids upscaled to 2.5° based on drought clusters from ERA5-Land third layer's soil moisture. Drought-prone areas quantified from ERA5-Land soil moisture (Fig. 8) are consistent to those listed in GDIS (Fig. 6). The Horn of Africa, northern China, and western India can also be recognized as drought-prone areas by ERA5-Land-based drought clusters. Mozambique cannot be identified as a drought-prone area in ERA5-Land. Please note that the number of the drought cluster centroids (Fig. 8) would be larger than the number of drought events in GDIS (Fig. 6). The number of drought events in GDIS is counted as one event even if a GDIS event lasts several months. On the other hand, the number of drought cluster centroids is counted in every monthly time step. Several clusters may be contained simultaneously in a large GDIS drought area. ERA5-Land identifies some drought-prone areas which are not included in GDIS, such as Namibia, Indonesia, and Spain. The locations of drought-prone areas are almost the same when drought clusters are generated by soil moisture in different soil layers (Fig. S2). The drought-prone areas are most distinguishable from their surroundings in the third layer case.

https://doi.org/10.5194/hess-2022-124
Preprint. Discussion started: 1 April 2022


Hydrology and Earth System Sciences
Discussions

5 Discussion

In previous studies, the verification of sub-national drought events by hydro-meteorological data has been insufficient. There are some works only on the specific regions (e.g., Bayissa et al., 2018; Lu et al., 2019) or in a short period of time (Sánchez et al., 2018), due to the lack of precise sub-national information on disaster locations. Using the latest sub-national disaster database, GDIS, this study was able to cover a large number of drought events compared to previous studies. In Sánchez et al. (2018), the criterion for the detection of drought events was that more than one-third of the area was under drought. However, the size of the drought event area could affect the criterion, and the threshold of one-third is rather subjective. By defining the standardized drought index, this study uniformly and objectively showed the accurate detection of sub-national drought information by ERA5-Land soil moisture, even if the size of the event differs.

The vulnerability to drought was quantitatively assessed across regions by comparing SDI. We confirmed that Sub-Saharan Africa and South Asia were vulnerable to drought, while North America and Europe were robust to drought. Previous studies have shown that higher GDP per capita is associated with lower vulnerability to natural hazards (e.g., Kim et al., 2019; Tanoue et al., 2016), and our finding is consistent with these previous works. There are global vulnerability indices such as the WorldRiskIndex (Welle and Birkmann, 2015), INFORM index (Marin-Ferrer et al., 2017), and ND-GAIN (Chen et al. 2015), which combine socio-economic factors such as economic level, infrastructure level, and education level. These indices have also indicated that Sub-Saharan Africa and South Asia are vulnerable, while North America, Europe, Australia, and Japan are robust to natural hazards (Birkmann et al., 2021; Birkmann et al., 2022; Garschagen et al., 2021). The reason why the low-income countries are vulnerable to drought could be the lack of drought mitigation measures (e.g., dams, irrigation system, early-warning system, etc.), as pointed out in previous studies (e.g., Lavell et al., 2012; Stringer et al., 2020; UNEP, 2018).

GDIS, a sub-national level disaster locations dataset, has enabled us to understand drought-prone areas on a finer scale than the previous global-scale analyses. EM-DAT is generally a national-level database with limited sub-national information. Shen and Hwang (2019) compared the frequency of disaster occurrence in EM-DAT at the national level and pointed out that frequent areas were large or populated countries. GDIS provides more detailed information about drought-prone areas, especially in large countries such as China and India. We successfully clarified that there was the considerable heterogeneity of the drought-prone areas within the country.

There were some inconsistencies between hydro-meteorological drought-prone areas in ERA5-Land and socio-economic drought-prone areas in GDIS. Mozambique is a socio-economic drought-prone area, which cannot be identified as a drought-prone area in ERA5-Land. Madagascar, which is geographically closer to Mozambique, is a drought-prone area in ERA5-Land. The lack of the reproducibility of ERA5-Land might affect these inconsistencies. In contrast, there were some hydro-

https://doi.org/10.5194/hess-2022-124
Preprint. Discussion started: 1 April 2022


Hydrology and Earth System Sciences
Discussions

meteorological drought-prone areas in ERA5-Land, which were not included in socio-economic drought-prone areas in GDIS (e.g., Spain, Namibia, and Indonesia). Spain, a member of European countries, is robust to drought, as shown in Fig. 5. In Namibia, a lack of exposure makes socio-economic droughts less likely to occur. When assessing socio-economic impact, the presence of the exposure should also be considered (Visser et al., 2014). Namibia has extremely low population density throughout the country (under 1 person per km^2 in 2020, Gridded Population of the World (GPW) version 4.11, Doxsey-Whitfield et al., 2015). Similarly, western Australia, central and eastern Russia do not have socio-economic droughts in GDIS due to the low population density. In Indonesia, the absolute amount of rainfall is so high that the relatively small soil moisture may not cause socio-economic drought. Kim et al. (2019) reported that there was no clear correlation between drought severity and yields reduction in areas where average annual precipitation is more than 900 mm. Indonesia is one of the rainiest regions on the globe, with more than 2,700 mm annual precipitation (2017, FAO). Despite these individual circumstances, our results showed that socio-economic drought-prone areas in GDIS were generally consistent with hydro-meteorological drought-prone areas in ERA5-Land (the Horn of Africa, northern China, and western India), indicating that the reanalysis product can be utilized to show a "potential" of socio-economic drought impact.

Although various reanalysis products have been developed and their reproducibility has been verified (e.g., Muñoz-Sabater et al., 2021; Reichle et al., 2017; Rodell et al., 2004), few studies have examined the reproducibility in terms of socio-economic impact. Sawada (2018) compared the areas identified as drought quantified from a reanalysis product with the disaster records from EM-DAT, but only in a country-scale. As seen in Fig. 7, national-level information does not provide accurate pictures of disaster locations, which is insufficient for validation data. The use of sub-national disaster databases such as GDIS opens the door to evaluate reanalysis products in terms of the disaster occurrence.

Although there are many variables to quantify hydro-meteorological droughts, we showed that soil moisture could clearly capture the GDIS drought events in time and space. In the comparison of the soil layers, deep layers (i.e., the third layer (28–100 cm) and root-zone layer (0–100 cm)) were affected for a longer period, which made SDI tend to be higher than that of the first (0–7 cm) and second (7–28 cm) layers during drought. In drought clustering, the drought-prone areas were most distinguishable from their surroundings in the third layer case. Sawada and Koike (2016) used land reanalysis products to confirm that drought propagates from surface to root-zone (5–100 cm) soil moisture and then to vegetation, and showed that root-zone soil moisture and vegetation were good indices to capture the prolonged drought impact in the case of the Horn of Africa drought (2010–2011). In this study, we confirmed that many of the serious socio-economic events such as those listed in GDIS were the events that were associated with the soil moisture deficit not only on the surface layer but also down to the root. Many drought studies have used root-zone soil moisture and our study has reinforced its validity. Hao and Singh (2015) suggested that a single drought index is insufficient to capture different impact types of droughts (e.g., water shortage, famine. wildfire, etc.). Several studies have tried to develop a new combined drought index based on several hydro-meteorological variables (e.g., precipitation and soil moisture) to express socio-economic impact by using Random Forest

https://doi.org/10.5194/hess-2022-124
Preprint. Discussion started: 1 April 2022

315 models (e.g., Bachmair et al., 2016; Hobeichi et al., 2022). Further studies are needed for the variable selection and drought indices according to the type of drought, which leads to more accurate representation of socio-economic impact by hydro-meteorological variables.

The limitation of the vulnerability assessment of this study is that we only captured the static conditions over time. We do 320 not reveal which factors (e.g., infrastructure, economic, social, or cultural assets) contribute to the vulnerability. Vulnerability to disasters is complex and dynamic. For example, people's water demand could dynamically change after experiencing drought events (Gonzales and Ajami, 2017). Improved irrigation scheduling (Cao et al., 2019) and dam operation (Wu et al., 2018) based on forecasts could reduce the drought damage. Although we quantified the vulnerability to drought in different geographical regions, detailed analyses are needed to reveal the complex and dynamic nature of 325 vulnerability based on the linkage between hydro-meteorological drought hazards and socio-economic impacts.

The major limitation of this study is the incompleteness of the drought impact data. Although GDIS enables sub-national drought analysis, GDIS only covers about 60% of droughts in EM-DAT (Rosvold and Buhaug, 2021). Note that even EM-DAT does not cover all disasters. Moreover, EM-DAT and GDIS have insufficient quantitative impact information. EM-330 DAT provides no information about the amount of damage in multiple drought events. There is a lot of uncertainty in the amount of damage because it is difficult to quantify indirect damages of drought (e.g., Yokomatsu et al., 2020). Although GDIS is a pioneering work to achieve the detailed analysis of the relationship between hydro-meteorological drought hazards and socio-economic impact of drought in a global scale, which we performed in this paper, there is much room for improvement of the global disaster database such as including detailed and quantifiable damage information by following the 335 approaches of EDII and US DIR.

6 Conclusions

We evaluated how the sub-national socio-economic drought events shown in GDIS could be reproduced by the natural hydrological drought indices generated by the reanalysis product, ERA5-Land. We confirmed that the reanalysis product captured the socio-economic impact at a statistically significant level. We also showed that Sub-Saharan Africa and South 340 Asia were vulnerable to drought, while North America and Europe were robust to drought. We analyzed the global spatial distribution of drought frequency, and we found that socio-economic drought-prone areas in GDIS were generally consistent with hydro-meteorological drought-prone areas expressed by soil moisture deficit (the Horn of Africa, northern China, and western India). The use of sub-national information, such as GDIS, makes it possible to identify socio-economic drought-prone areas on a finer scale and can contribute to validating reanalysis products.

https://doi.org/10.5194/hess-2022-124
Preprint. Discussion started: 1 April 2022


Hydrology and Earth System Sciences
Discussions

345 **Code and data availability**

The drought clustering python code can be downloaded at https://github.com/julherest/drought_clusters (last access: 31 March 2022). The ERA5-Land dataset can be downloaded at https://cds.climate.copernicus.eu/cdsapp#!/dataset/reanalysis-era5-land?tab=form (last access: 31 March 2022). The GDIS dataset can be downloaded at https://cmr.earthdata.nasa.gov/search/concepts/C2022273992-SEDAC.html (last access: 31 March 2022). The EM-DAT
350 database can be vied at https://www.emdat.be/ (last access: 31 March 2022). World bank's geographical regions can be vied at https://datatopics.worldbank.org/world-development-indicators/the-world-by-income-and-region.html (last access: 31 March 2022). The MODIS land cover data can be downloaded at https://lpdaac.usgs.gov/products/mcd12c1v006/ (last access: 31 March 2022). The gridded population of the world can be downloaded at https://sedac.ciesin.columbia.edu/data/set/gpw-v4-population-density-rev11 (last access: 31 March 2022). The global map of
355 FAO's annual average precipitation can be vied at World bank website https://data.worldbank.org/indicator/ag.lnd.prcp.mm?msclkid=215b9959b08711ec944832810373c8aa&view=map (last access: 31 March 2022).

Author contribution

Y.S. and Y.K. designed the experiments and Y.K. carried them out. Y.K. prepared the manuscript with contributions from
360 Y.S. Y.S. acquired the funding.

Competing interests

The authors declare that they have no conflict of interest.

Acknowledgements

This work was supported by JAXA grant (ER2GWF102 and ER3AMF106), JSPS KAKENHI grant (21H01430), and Katsu
365 Kimura Research Award.

References

Almendra-Martín, L., Martínez-Fernández, J., González-Zamora, A., Benito-Verdugo, P., and Herrero-Jiménez, C. M.: Agricultural Drought Trends on the Iberian Peninsula: An Analysis Using Modeled and Reanalysis Soil Moisture Products, Atmosphere, 12, https://doi.org/10.3390/atmos12020236, 2021.

https://doi.org/10.5194/hess-2022-124
Preprint. Discussion started: 1 April 2022

Andreadis, K. M., Clark, E. A., Wood, A. W., Hamlet, A. F., and Lettenmaier, D. P.: Twentieth-century drought in the conterminous United States, J. Hydrometeorol., 6, 985–1001, https://doi.org/10.1175/JHM450.1, 2005.

Bachmair, S., Svensson, C., Hannaford, J., Barker, L. J., and Stahl, K.: A quantitative analysis to objectively appraise drought indicators and model drought impacts, Hydrol. Earth Syst. Sci., 20, 2589–2609, https://doi.org/10.5194/hess-20-2589-2016, 2016.

Bayissa, Y., Maskey, S., Tadesse, T., van Andel, S. J., Moges, S., van Griensven, A., and Solomatine, D.: Comparison of the Performance of Six Drought Indices in Characterizing Historical Drought for the Upper Blue Nile Basin, Ethiopia, Geosciences, 8, https://doi.org/10.3390/geosciences8030081, 2018.

Birkmann, J., Feldmeyer, D., McMillan, J. M., Solecki, W., Totin, E., Roberts, D., Trisos, C., Jamshed, A., Boyd, E., and Wrathall, D.: Regional clusters of vulnerability show the need for transboundary cooperation, Environ. Res. Lett., 16, https://doi.org/10.1088/1748-9326/ac1f43, 2021.

Birkmann, J., Jamshed, A., McMillan, J. M., Feldmeyer, D., Totin, E., Solecki, W., Ibrahim, Z. Z., Roberts, D., Kerr, R. B., Poertner, H. O., Pelling, M., Djalante, R., Garschagen, M., Filho, W. L., Guha-Sapir, D., and Alegria, A.: Understanding human vulnerability to climate change: A global perspective on index validation for adaptation planning, Sci. Total Environ., 803, https://doi.org/10.1016/j.scitotenv.2021.150065, 2022.

Cao, J. J., Tan, J. W., Cui, Y. L., and Luo, Y. F.: Irrigation scheduling of paddy rice using short-term weather forecast data, Agr. Water Manage., 213, 714–723, https://doi.org/10.1016/j.agwat.2018.10.046, 2019.

Carrão, H., Naumann, G., and Barbosa, P.: Mapping global patterns of drought risk: An empirical framework based on sub-national estimates of hazard, exposure and vulnerability, Global Environ. Chang, 39, 108–124, https://doi.org/10.1016/j.gloenvcha.2016.04.012, 2016.

Chen, C., Noble, I., Hellmann, J., Coffee, J., Murillo, M., Chawla, N.: University of Notre Dame Global Adaptation Index Country Index Technical Report, University of Notre Dame, South Bend, USA, 2015.

Chen, Z. F., Wang, W. G., Yu, Z. B., Xia, J., and Schwartz, F. W.: The collapse points of increasing trend of vegetation rain-use efficiency under droughts, Environ. Res. Lett., 15, https://doi.org/10.1088/1748-9326/abb332, 2020.

de Brito, M. M., Kuhlicke, C., and Marx, A.: Near-real-time drought impact assessment: a text mining approach on the 2018/19 drought in Germany, Environ. Res. Lett., 15, https://doi.org/10.1088/1748-9326/aba4ca, 2020.

Doxsey-Whitfield, E., MacManus, K., Adamo, S. B., Pistolesi, L., Squires, J., Borkovska, O., and Baptista, S. R.: Taking advantage of the improved availability of census data: a first look at the gridded population of the world, version 4, Pap. Appl. Geogr., 1, 226–234, https://doi.org/10.1080/23754931.2015.1014272, 2015.

Friedl, M. and Sulla-Menashe, D.: MCD12C1 MODIS/Terra+Aqua Land Cover Type Yearly L3 Global 0.05Deg CMG V006, NASA EOSDIS Land Processes DAAC [data set], https://doi.org/10.5067/MODIS/MCD12C1.006, 2015.

Fuchs, S., Keiler, M., Ortlepp, R., Schinke, R., and Papathoma-Kohle, M.: Recent advances in vulnerability assessment for the built environment exposed to torrential hazards: Challenges and the way forward, J. Hydrol., 575, 587–595, https://doi.org/10.1016/j.jhydrol.2019.05.067, 2019.

https://doi.org/10.5194/hess-2022-124
Preprint. Discussion started: 1 April 2022

Garschagen, M., Doshi, D., Reith, J., and Hagenlocher, M.: Global patterns of disaster and climate risk-an analysis of the consistency of leading index-based assessments and their results, Climatic Change, 169, https://doi.org/10.1007/s10584-021-03209-7, 2021.

Gonzales, P. and Ajami, N.: Social and Structural Patterns of Drought-Related Water Conservation and Rebound, Water Resour. Res., 53, 10619–10634, https://doi.org/10.1002/2017wr021852, 2017.

Guha-Sapir, D., Below, R., and Hoyois, P. H.: EM-DAT: International Disaster Database, Université Catholique de Louvain, Brussels, Belgium, http://www.emdat.be, last access: 31 March 2022.

Hanel, M., Rakovec, O., Markonis, Y., Maca, P., Samaniego, L., Kysely, J., and Kumar, R.: Revisiting the recent European droughts from a long-term perspective, Sci. Rep., 8, https://doi.org/10.1038/s41598-018-27464-4, 2018.

Hao, Z. C. and Singh, V. P.: Drought characterization from a multivariate perspective: A review, J. Hydrol., 527, 668–678, https://doi.org/10.1016/j.jhydrol.2015.05.031, 2015.

Herrera-Estrada, J. E. and Diffenbaugh, N. S.: Landfalling Droughts: Global Tracking of Moisture Deficits From the Oceans Onto Land, Water Resour. Res., 56, https://doi.org/10.1029/2019wr026877, 2020.

Herrera-Estrada, J. E., Satoh, Y., and Sheffield, J.: Spatiotemporal dynamics of global drought, Geophys. Res. Lett., 44, 2254–2263, https://doi.org/10.1002/2016gl071768, 2017.

Hobeichi, S., Abramowitz, G., Evans, J. P., and Ukkola, A.: Toward a Robust, Impact-Based, Predictive Drought Metric, Water Resour. Res., 58, https://doi.org/10.1029/2021wr031829, 2022.

Jägermeyr, J. and Frieler, K.: Spatial variations in crop growing seasons pivotal to reproduce global fluctuations in maize and wheat yields, Sci. Adv., 4, https://doi.org/10.1126/sciadv.aat4517, 2018.

Kim, W., Iizumi, T., and Nishimori, M.: Global Patterns of Crop Production Losses Associated with Droughts from 1983 to 2009, J. Appl. Meteorol. Clim., 58, 1233–1244, https://doi.org/10.1175/jamc-d-18-0174.1, 2019.

Lavell, A., Oppenheimer, M., Diop, C., Hess, J., Lempert, R., Li, J. P., Muir-Wood, R., Myeong, S., Moser, S., Takeuchi, K., Cardona, O. D., Hallegatte, S., Lemos, M., Little, C., Lotsch, A., and Weber, E., Field, C. B., Barros, V., Stocker, T. F., Dahe, Q., Dokken, D. J., Ebi, K. L., Mastrandrea, M. D., Mach, K. J., Plattner, G. K., Allen, S. K., Tignor, M., and Midgley, P. M. (Eds.): Climate Change: New Dimensions in Disaster Risk, Exposure, Vulnerability, and Resilience, Managing the Risks of Extreme Events and Disasters to Advance Climate Change Adaptation: Special Report of the Intergovernmental Panel on Climate Change, Cambridge University Press, Cambridge, UK/New York, 25–64, https://doi.org/10.1017/CBO9781139177245.004, 2012.

Lu, J., Jia, L., Zhou, J., Zheng, C., and Hu, G.: Adaptablity of Six Global Drought Indices Over China, IEEE International Geoscience and Remote Sensing Symposium (IGARSS), Yokohama, JAPAN, 28 July–02 August 2019, 9922–9925, https://doi.org/10.1109/IGARSS.2019.8899184, 2019.

Marin-Ferrer, M., Vernaccini, L., and Poljanšek, K.: Index for Risk Management - INFORM: Concept and Methodology, Version 2017, Joint Research Center of European Commission, Luxembourg, 2017.

https://doi.org/10.5194/hess-2022-124
Preprint. Discussion started: 1 April 2022

Massey, F. J.: The Kolmogorov-Smirnov Test for Goodness of Fit, J. Am. Stat. Assoc., 46, 68–78, https://doi.org/10.2307/2280095, 1951.

McKee, T. B., Doesken, N. J., and Kleist, J.: The relationship of drought frequency and duration to time scales, Preprints, 8th Conference on Applied Climatology, Climatology, Anaheim, California, 17–22 January 1993, 179–184, 1993.

Mishra, A. K. and Singh, V. P.: A review of drought concepts, J. Hydrol., 391, 204–216, https://doi.org/10.1016/j.jhydrol.2010.07.012, 2010.

Mocko, D. M., Kumar, S. V., Peters-Lidard, C. D., and Wang, S. G.: Assimilation of Vegetation Conditions Improves the Representation of Drought over Agricultural Areas, J. Hydrometeorol., 22, 1085–1098, https://doi.org/10.1175/JHM-D-20-0065.1, 2021.

Muñoz Sabater, J.: ERA5-Land monthly averaged data from 1981 to present, Copernicus Climate Change Service (C3S) Climate Data Store (CDS) [data set], https://doi.org/10.24381/cds.68d2bb3, 2019.

Muñoz Sabater, J.: ERA5-Land monthly averaged data from 1950 to 1980, Copernicus Climate Change Service (C3S) Climate Data Store (CDS) [data set], https://doi.org/10.24381/cds.68d2bb3, 2021.

Munoz-Sabater, J., Dutra, E., Agusti-Panareda, A., Albergel, C., Arduini, G., Balsamo, G., Boussetta, S., Choulga, M., Harrigan, S., Hersbach, H., Martens, B., Miralles, D. G., Piles, M., Rodriguez-Fernandez, N. J., Zsoter, E., Buontempo, C., and Thepaut, J. N.: ERA5-Land: a state-of-the-art global reanalysis dataset for land applications, Earth Syst. Sci. Data, 13, 4349–4383, https://doi.org/10.5194/essd-13-4349-2021, 2021.

Noel, M., Bathke, D., Fuchs, B., Gutzmer, D., Haigh, T., Hayes, M., Podebradska, M., Shield, C., Smith, K., and Svoboda, M.: Linking Drought Impacts to Drought Severity at the State Level, B. Am. Meteorol. Soc., 101, 1312–1321, https://doi.org/10.1175/bams-d-19-0067.1, 2020.

Reichle, R. H., Draper, C. S., Liu, Q., Girotto, M., Mahanama, S. P. P., Koster, R. D., and De Lannoy, G. J. M.: Assessment of MERRA-2 Land Surface Hydrology Estimates, J. Climate, 30, 2937–2960, https://doi.org/10.1175/jcli-d-16-0720.1, 2017.

Rodell, M., Houser, P. R., Jambor, U., Gottschalck, J., Mitchell, K., Meng, C. J., Arsenault, K., Cosgrove, B., Radakovich, J., Bosilovich, M., Entin, J. K., Walker, J. P., Lohmann, D., and Toll, D.: The global land data assimilation system, B. Am. Meteorol. Soc., 85, 381–394, https://doi.org/10.1175/bams-85-3-381, 2004.

Rosvold, E. L. and Buhaug, H.: GDIS, a global dataset of geocoded disaster locations, Sci. Data, 8, https://doi.org/10.1038/s41597-021-00846-6, 2021.

Sánchez, N., González-Zamora, Á., Martínez-Fernández, J., Piles, M., and Pablos, M.: Integrated remote sensing approach to global agricultural drought monitoring, Agr. Forest Meteorol., 259, 141–153, https://doi.org/10.1016/j.agrformet.2018.04.022, 2018.

Sawada, Y.: Quantifying Drought Propagation from Soil Moisture to Vegetation Dynamics Using a Newly Developed Ecohydrological Land Reanalysis, Remote Sens., 10, https://doi.org/10.3390/rs10081197, 2018.

https://doi.org/10.5194/hess-2022-124
Preprint. Discussion started: 1 April 2022

Sawada, Y. and Koike, T.: Towards ecohydrological drought monitoring and prediction using a land data assimilation system: A case study on the Horn of Africa drought (2010–2011), J. Geophys. Res. Atmos., 121, 8229–8242, https://doi.org/10.1002/2015jd024705, 2016.

Schulzweida, U.: CDO User Guide (Version 2.0.0), Zenodo [software], http://doi.org/10.5281/zenodo.5614769, 2021.

Sheffield, J. and Wood, E. F.: Drought: past problems and future scenarios, 1st Edition, Routledge, London, UK, https://doi.org/10.4324/9781849775250, 2011.

Shen, G. Q. and Hwang, S. N.: Spatial-Temporal snapshots of global natural disaster impacts Revealed from EM-DAT for 1900–2015, Geomat. Nat. Haz. Risk, 10, 912–934, https://doi.org/10.1080/19475705.2018.1552630, 2019.

Skamarock, W. C.: Evaluating mesoscale NWP models using kinetic energy spectra, Mon. Weather Rev., 132, 3019–3032, https://doi.org/10.1175/mwr2830.1, 2004.

Stahl, K., Kohn, I., Blauhut, V., Urquijo, J., De Stefano, L., Acacio, V., Dias, S., Stagge, J. H., Tallaksen, L. M., Kampragou, E., Van Loon, A. F., Barker, L. J., Melsen, L. A., Bifulco, C., Musolino, D., de Carli, A., Massarutto, A., Assimacopoulos, D., and Van Lanen, H. A. J.: Impacts of European drought events: insights from an international database of text-based reports, Nat. Hazards Earth Syst. Sci., 16, 801–819, https://doi.org/10.5194/nhess-16-801-2016, 2016.

Stringer, L. C., Fraser, E. D. G., Harris, D., Lyon, C., Pereira, L., Ward, C. F. M., and Simelton, E.: Adaptation and development pathways for different types of farmers, Environ. Sci. Policy, 104, 174–189, https://doi.org/10.1016/j.envsci.2019.10.007, 2020.

Svoboda, M., LeComte, D., Hayes, M., Heim, R., Gleason, K., Angel, J., Rippey, B., Tinker, R., Palecki, M., Stooksbury, D., Miskus, D., and Stephens, S.: The drought monitor, B. Am. Meteorol. Soc., 83, 1181–1190, https://doi.org/10.1175/1520-0477-83.8.1181, 2002.

Tanoue, M., Hirabayashi, Y., and Ikeuchi, H.: Global-scale river flood vulnerability in the last 50 years, Sci. Rep., 6, https://doi.org/10.1038/srep36021, 2016.

Trnka, M., Hlavinka, P., Možný, M., Semerádová, D., Štěpánek, P., Balek, J., Bartošová, L., Zahradníček, P., Bláhová, M., Skalák, P., Farda, A., Hayes, M., Svoboda, M., Wagner, W., Eitzinger, J., Fischer, M., and Žalud, Z.: Czech Drought Monitor System for monitoring and forecasting agricultural drought and drought impacts, Int. J. Climatol., 40, 5941–5958, https://doi.org/10.1002/joc.6557, 2020.

Tschumi, E. and Zscheischler, J.: Countrywide climate features during recorded climate-related disasters, Climatic Change, 158, 593–609, https://doi.org/10.1007/s10584-019-02556-w, 2020.

Udmale, P., Ichikawa, Y., Ning, S. W., Shrestha, S., and Pal, I.: A statistical approach towards defining national-scale meteorological droughts in India using crop data, Environ. Res. Lett., 15, https://doi.org/10.1088/1748-9326/abacfa, 2020.

UNDP: Reducing Disaster Risk: A Challenge for Development, United Nations Development Programme (UNDP), New York, USA, 2004.

https://doi.org/10.5194/hess-2022-124
Preprint. Discussion started: 1 April 2022

UNEP: The Adaptation Gap Report 2018, United Nations Environment Programme (UNEP), Nairobi, Kenya, 2018.

Vicente-Serrano, S. M., Beguería, S., and López-Moreno, J. I.: A Multiscalar Drought Index Sensitive to Global Warming: The Standardized Precipitation Evapotranspiration Index, J. Climate, 23, 1696–1718, https://doi.org/10.1175/2009jcli2909.1, 2010.

Visser, H., Petersen, A. C., and Ligtvoet, W.: On the relation between weather-related disaster impacts, vulnerability and climate change, Climatic Change, 125, 461–477, https://doi.org/10.1007/s10584-014-1179-z, 2014.

Welle, T. and Birkmann, J.: The World Risk Index – An Approach to Assess Risk and Vulnerability on a Global Scale, J. Extr. Even., 02, 1550003, https://doi.org/10.1142/S2345737615500037, 2015.

Wilhite, D. A. and Glantz, M. H.: Understanding: the drought phenomenon: the role of definitions, Water Int., 10, 111–120, https://doi.org/10.1080/02508068508686328, 1985.

Wilhite, D. A., Svoboda, M. D., and Hayes, M. J.: Understanding the complex impacts of drought: A key to enhancing drought mitigation and preparedness, Water Resour. Manag., 21, 763–774, https://doi.org/10.1007/s11269-006-9076-5, 2007.

Wu, J. F., Liu, Z. Y., Yao, H. X., Chen, X. H., Chen, X. W., Zheng, Y. H., and He, Y. H.: Impacts of reservoir operations on multi-scale correlations between hydrological drought and meteorological drought, J. Hydrol., 563, 726–736, https://doi.org/10.1016/j.jhydrol.2018.06.053, 2018.

Yokomatsu, M., Ishiwata, H., Sawada, Y., Suzuki, Y., Koike, T., Naseer, A., and Cheema, M. J. M.: A multi-sector multi-region economic growth model of drought and the value of water: A case study in Pakistan, Int. J. Disast. Risk Re., 43, https://doi.org/10.1016/j.ijdrr.2019.101368, 2020.

Zink, M., Samaniego, L., Kumar, R., Thober, S., Mai, J., Schäfer, D., and Marx, A.: The German drought monitor, Environ. Res. Lett., 11, https://doi.org/10.1088/1748-9326/11/7/074002, 2016.

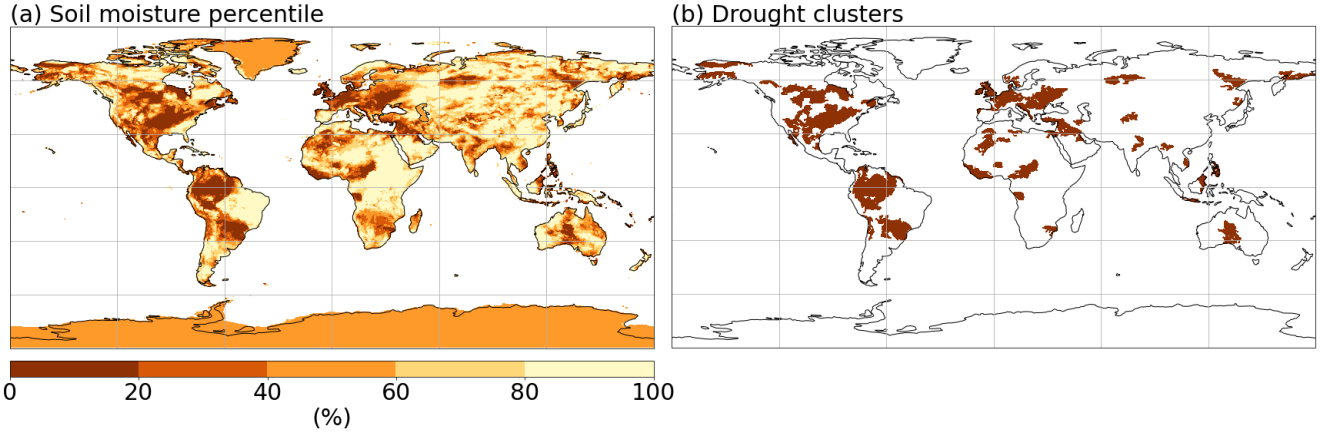

Figure 1: Demonstration of drought clustering. (a) Global map of soil moisture percentile for the root-zone layer's soil moisture in January 1964. (b) Drought clusters, spatially contiguous areas under drought (below 20th percentile) are extracted from (a). A 2-D median filter is applied prior to drought clustering, which makes slight differences compared with (a).

https://doi.org/10.5194/hess-2022-124
Preprint. Discussion started: 1 April 2022

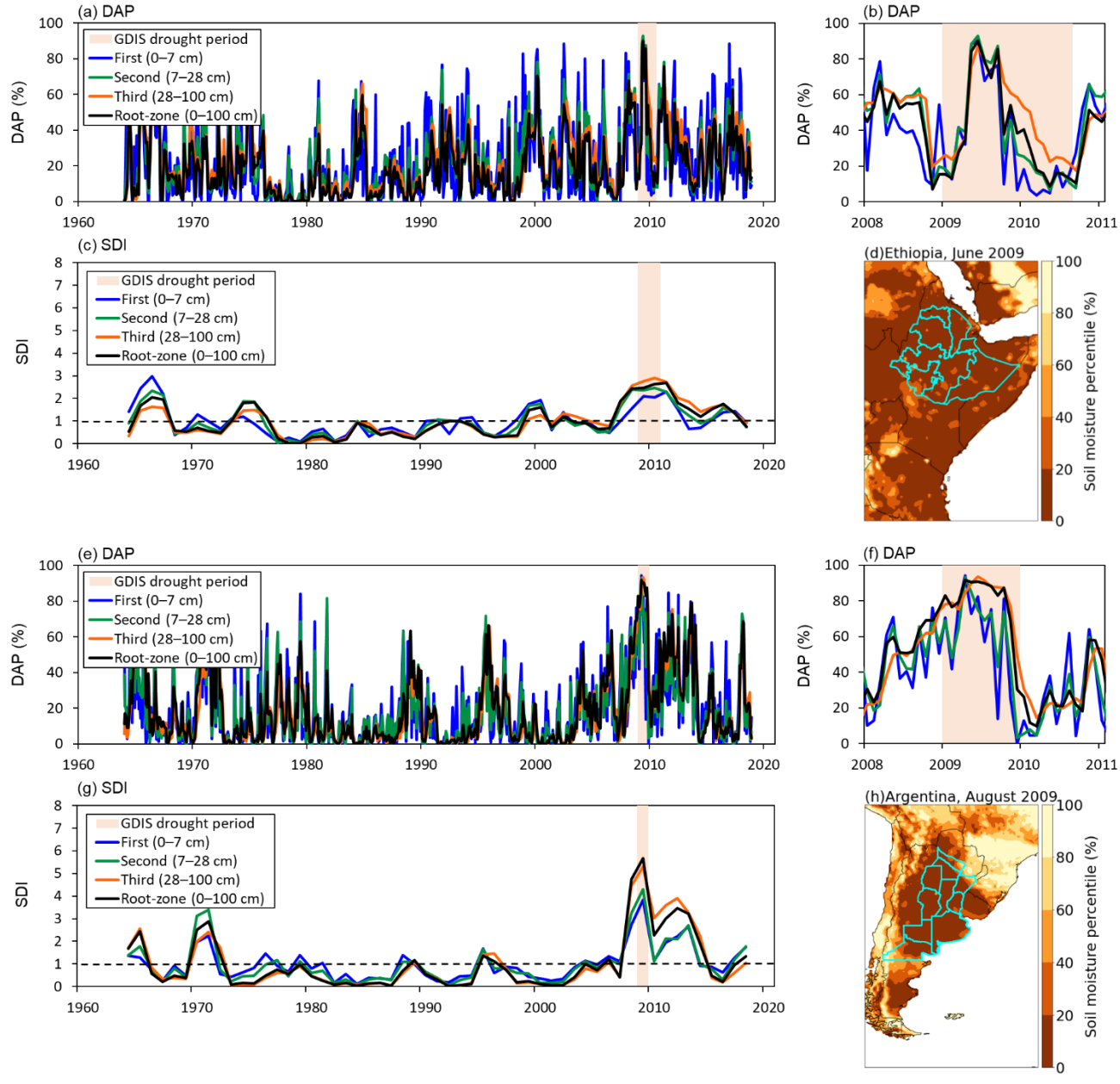

Figure 2: Demonstration of drought indices in different soil layers for the drought events in Ethiopia in 2009 (a–d) and Argentina in 2009 (e–h). (a, e) DAP; red band shows the GDIS drought period, and each coloured line shows the values in each soil layer (first (blue), second (green), third (orange), and root-zone (black)). (b, f) the enlarged view of DAP around the GDIS drought period. (c, g) SDI; the legends are the same as DAP (a, e), and grey dotted line shows the value of 1 (the mean of SDI over the study period). (d, h) the GDIS drought area of this event; black line shows the country border, and light blue line shows the affected administrative units shown in GDIS. GDIS provides GIS polygons of administrative units, and administrative units with the same event identifier (*disasterno*) were treated as one "GDIS event area", the assembles of each light-blued administrative unit. The soil moisture percentile is generated from the root-zone layer's soil moisture as an example.

https://doi.org/10.5194/hess-2022-124
Preprint. Discussion started: 1 April 2022

Hydrology and Earth System Sciences
Discussions
Open Access
EGU

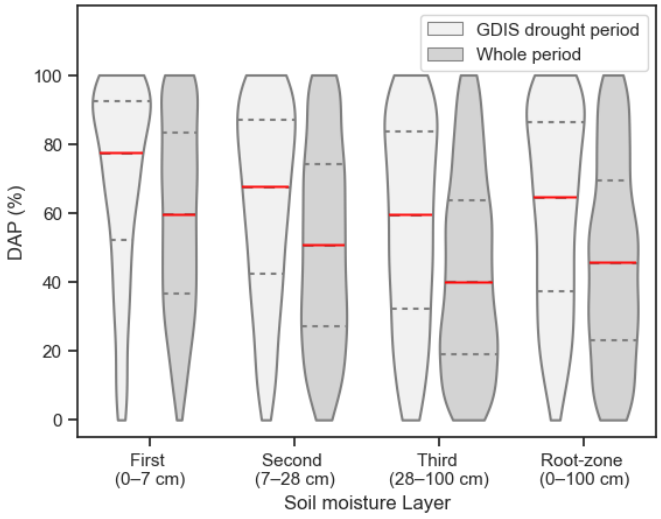

Figure 3: Comparison of DAP between the GDIS drought period and the whole period. The red line shows the median value and grey dotted lines show the 25th and 75th percentile values of each distribution.

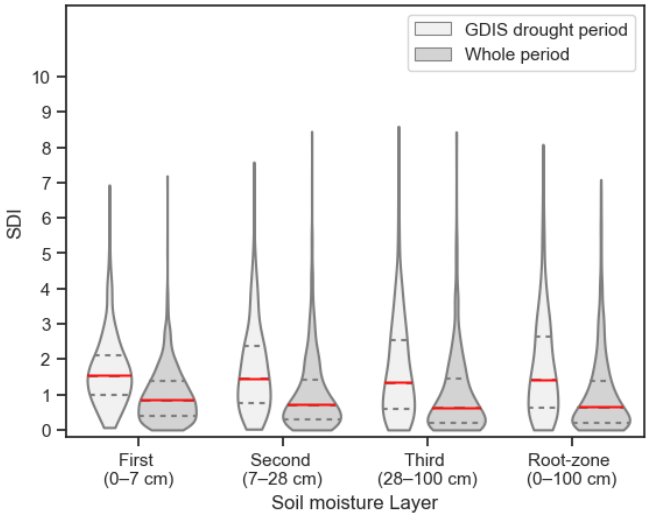

Figure 4: Comparison of SDI between the GDIS drought period and the whole period. The red line shows the median value and grey dotted lines show the 25th and 75th percentile values of each distribution.

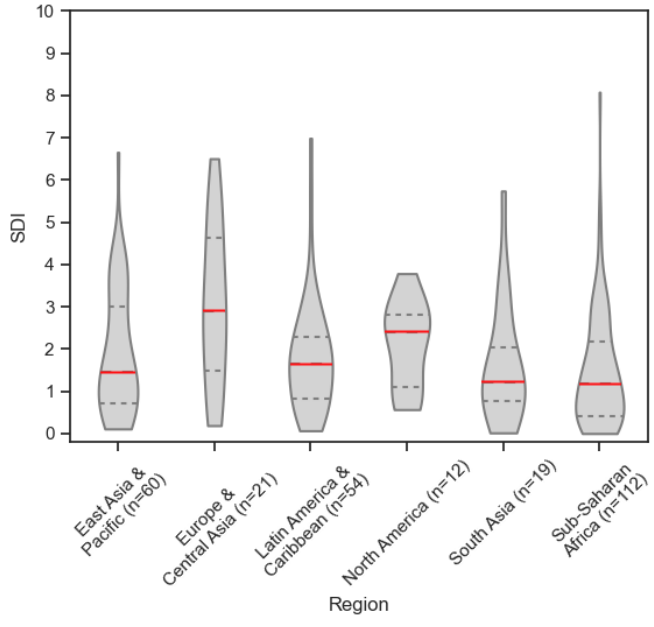

Figure 5: Comparison of the root-zone SDI by geographical regions. The red line shows the median value and grey dotted lines show the 25th and 75th percentile values of each distribution.

https://doi.org/10.5194/hess-2022-124
Preprint. Discussion started: 1 April 2022

Hydrology and Earth System Sciences
Discussions

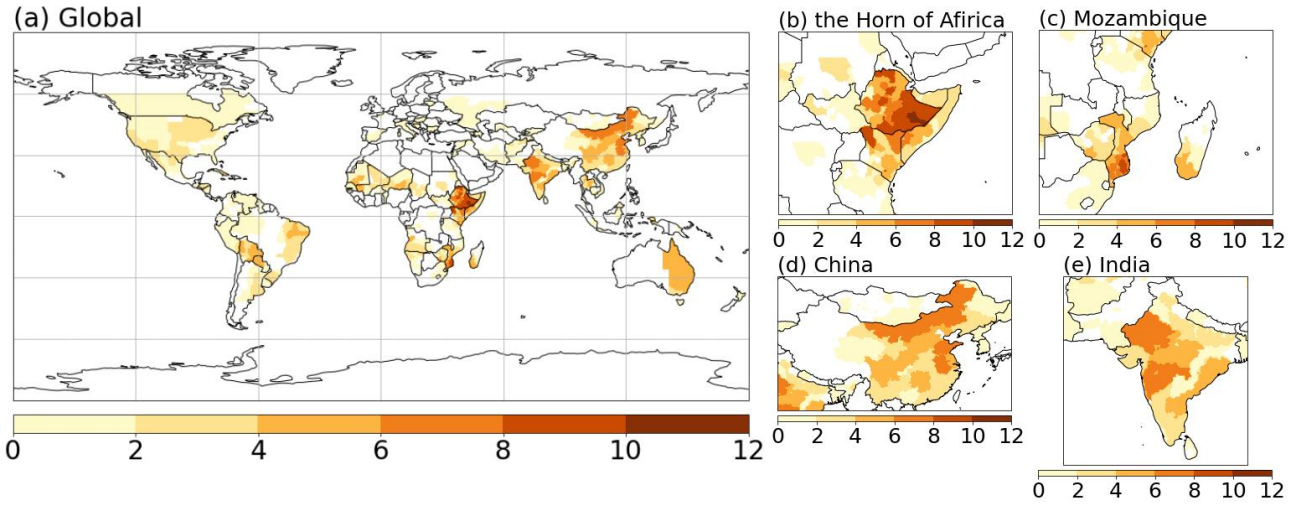

Figure 6: The number of drought events based on GDIS. (a) Global map, enlarged view of (b) the Horn of Africa, (c) Mozambique, (d) China, and (e) India.

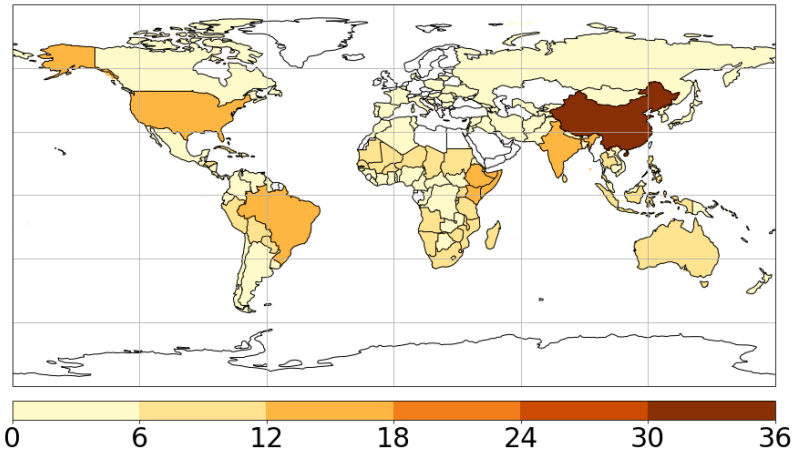

Figure 7: The number of drought events based on EM-DAT.

https://doi.org/10.5194/hess-2022-124
Preprint. Discussion started: 1 April 2022

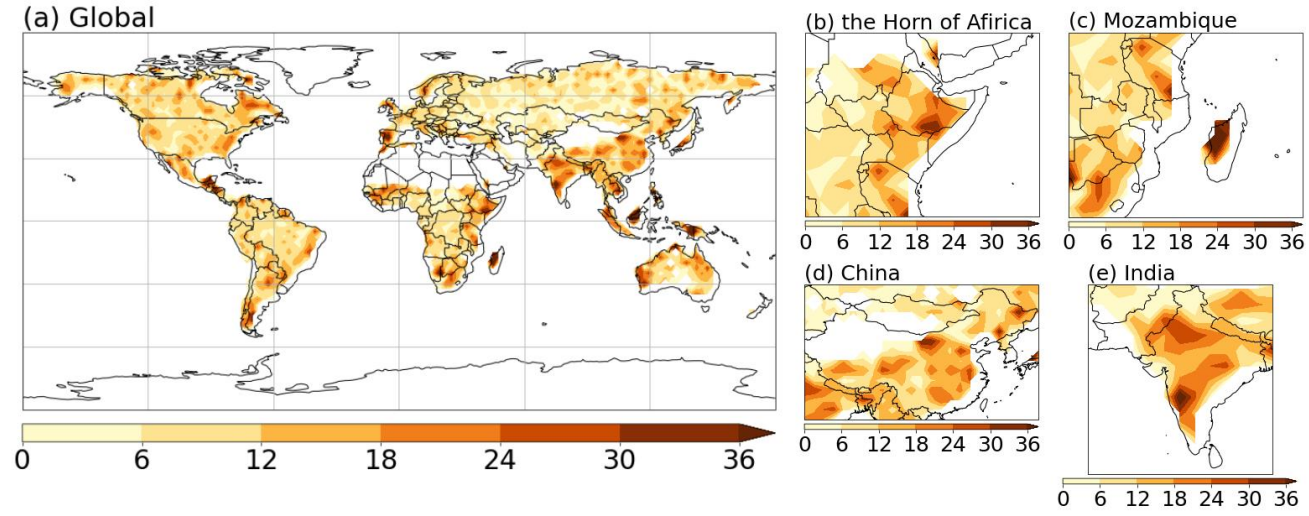

Figure 8: The number of drought cluster centroids based on ERA5-Land. (a) Global map, enlarged view of (b) the Horn of Africa, (c) Mozambique, (d) China, and (e) India.

530